

# Ice flow across the grounding line of the East Antarctic Ice Sheet between 80°E and 130°E

Chad A. Greene

December 1, 2012

## Abstract

Ice thickness, velocity, and bed elevation along the grounding line of outlet glaciers can control the flow of ice up to hundreds of kilometers inland. Here, surface elevation, bed elevation, surface velocity, and grounding line data sets are combined using ArcGIS to survey the geometries of coastal Antarctic ice streams in the region of 80°E to 130°E. Results show fair agreement with values calculated Pritchard *et al.* (Ref. [2]), but do not appear to support their claim that ice is thinning primarily where ice is thickest.

## 1 Background

The East Antarctic Ice Sheet (EAIS) has long been considered stable, but thinning downstream of the grounding zones of several EAIS outlet glaciers has recently been reported [1, 2]. Grounding zones are thought to act as flux gates which govern the flow of ice from land to sea, and the geometry of a glacier along its grounding line has important implications for upstream flow speed, downstream thinning rates, and the capacity of an ice mass to produce glacial earthquakes [2, 3]. Several nuanced interpretations exist for the term “grounding line,” but for the purposes of this paper it is defined simply as the location at which coastal ice transitions from resting on the continental bed to floating as an ice shelf.

Despite a significant research focus on West Antarctic glacial dynamics in recent decades, East Antarctica has largely escaped the attention of glaciologists. The present work is aimed at surveying the geometric properties, flow rates, and nominal bed elevations of East Antarctic grounding zones between 80°E and 130°E. The results of this study may be used to help prioritize research targets in the area. The focus area of this study is shown in Fig. 1.

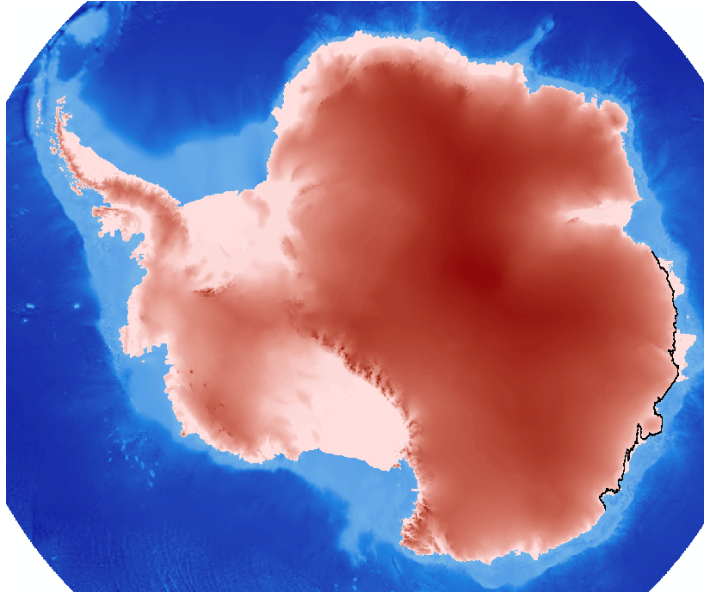


Figure 1: Antarctic ice surface elevation symbolized in white-to-red color scale and bed elevation shown as blue-to-white with increasing elevation. Clipped grounding line shown in black.

## 2 Data sources and preprocessing

This work required data sets containing ice surface elevation, ice bed elevation, ice velocity, and grounding line locations. For context, a data set containing glacier names in the region of interest was also included in this work.

### 2.1 Surface and bed elevation data

An attempt was made to generate ArcGIS digital elevation models for ice surface and bed elevations using a freely-available ASCII data set provided by the National Snow and Ice Data Center (NSIDC) [4]. The data set was easily loaded into MATLAB and saved as an ArcGIS-readable csv file by the following code:

```
demdat = urlread('ftp://sidacs.colorado.edu/pub/DATASETS/...  
BAMBER_DEM/bamber.5km97.dat');  
formatted_dem = [demdat(:,2) demdat(:,1) demdat(:,3)];  
csvwrite('surf_elev_dem.csv',formatted_dem);
```

The elevation data was loaded into ArcGIS using the ASCII 3D to Feature Class tool. Difficulties relating to declaration of the coordinate system made this data set too temperamental to use, so the backup plan of using shapefiles provided in Lab 6 of this course was implemented. The shapefiles were made available by Mark Helper, provided by the BEDMAP project and Scientific Committee on Antarctic Research (SCAR).

## 2.2 Ice velocity data

The MEaSUREs InSAR-Based Antarctica Ice Velocity Map is freely available from NSIDC as a NetCDF file with 900 m resolution [5].

## 2.3 Grounding line data

Three sources of grounding line data were found, each distributed through the NSIDC. The Brunt et al. (Ref. [6]) ICESat-derived grounding zones looked promising and straightforward as ASCII data containing latitudes and longitudes of the Antarctic grounding zones. Unfortunately, after importing these data into ArcGIS, it was evident that they were too spatially sparse to conduct an adequate survey of East Antarctic glaciers.

A second data set with high spatial resolution also came in the form of an ASCII file containing latitudes and longitudes of the grounding line [7]. At 168 MB, it was beneficial to clip the data to cover only the area of interest. The file was too large to be loaded into Microsoft Excel, so the following MATLAB script was generated to clip the data and convert it into an ArcGIS-readable format.

```
GL = fopen('InSAR-GL-Antarctica.txt');
GLd = textscan(GL, '%n %n %*[\n]');
fclose(GL);
lat = GLd{1};
lon = GLd{2};
lat=lat(lon>=80&lon<=130); % clip latitudes
lon=lon(lon>=80&lon<=130); % clip longitudes
GL = [lat lon];
xlswrite('InSAR-GL.xlsx', [lat lon]);
```

Again, after importing this data set into ArcGIS, it became evident that although the spatial resolution of this data set is sufficient for analysis within certain regions, the spatial coverage was insufficient for the goals of this study. A third data set was found in the convenient form of an ArcGIS shapefile with supporting databases [8]. The only

trick to importing the shapefile into ArcGIS, is the somewhat unintuitive step of setting the spatial reference for the layer to unprojected WGS84 geographic coordinates.

## **2.4 Feature name data**

Names and locations of glaciers in the region of interest were downloaded from the SCAR Composite Gazetteer (Ref. [9]) using the free online data download tool. Spatial coordinates and glacial features were selected and output to Microsoft Excel format. Several redundancies existed in the resulting file, so duplicate feature rows were deleted manually.

# **3 Procedure for ArcGIS analysis**

The procedure for data analysis in ArcGIS was as follows:

## **3.1 Set layer spatial reference**

The spatial reference was set to the SCAR stereographic projection with a standard parallel at 71°S.

## **3.2 Import surface and bed elevation layers**

The layers `bed_elev` and `surf_elev` were provided in raster format and easily imported by dragging-and-dropping from ArcCatalog into ArcMap. The surface was ordered above the bed. The surface layer was symbolized with a white-to-red color scale and bed elevation shown as blue-to-white with increasing elevation. Surface raster cells with zero values were set to 100% transparency.

## **3.3 Import and georeference ice velocity**

Ice velocity data were loaded into ArcGIS using the “Make NetCDF Raster Layer” tool. A raster layer was created for the  $x$ -component of ice velocity, and a second raster layer was created for the  $y$ -component of ice velocity. In this analysis, ice flow is assumed to flow locally perpendicular to the grounding line. Further, an approximation of plug

flow is made. With these approximations, the direction of ice motion was neglected and its speed was taken as

$$|v_{ij}| = \sqrt{v_{x,ij}^2 + v_{y,ij}^2}. \quad (1)$$

This was easily calculated in ArcMap using the raster calculator with the argument

`SquareRoot (Square ("vx_Layer1") + Square ("vy_Layer1"))`.

Surprisingly, the publicly-available `Antarctica_ice_velocity.nc` file is provided without spatial reference information embedded into the netCDF file. Supporting documentation published online states that the file includes an  $x$ -velocity map and a  $y$ -velocity map at 900 m resolution. An error map is also included, but not used in the current study. Supporting documentation states that the map was produced in South Pole Stereographic projection with a standard parallel at 71°S, matching the SCAR projection used in the current study. Velocity raster files were imported into ArcMap without any spatial reference, so after the speed map was calculated with using Map Algebra, it was georeferenced with 5 points and rectified using nearest neighbor interpolation, no compression, and points containing no data set to zero. The resulting raster had a cell size of 902.4 m, closely matching the published 900 m resolution. The rectification process is shown in the appendix in Fig. 5 and Fig. 6.

### 3.4 Import, clip, and measure properties along the grounding line

The grounding line shapefile contained over three million data points. To reduce computation times, grounding line points outside the longitudinal range of interest were eliminated. A simple SQL query could be performed to select only the points in the range of 80°E to 130°E, however the attribute table in the given grounding line shapefile contained latitudes and longitudes formatted as strings, meaning the SQL mathematical operators  $\geq$  and  $\leq$  would not work. To work around this issue, in the attribute table for the grounding line points, two new fields were added, both declared as doubles. The fields were named “lat” and “lon” and the field calculator was used to populate the columns with the Python commands `float( !Latitude! )` and `float( !Longitude! )`, respectively. The grounding line attribute table then contained columns for the numeric values of latitude and longitude.

Next, a new layer was created, containing only the values in the desired longitudinal range with the SQL query `"lon" >= 80 and "lon" <= 130`. This layer still contained more than 300,000 points and far exceeded the spatial resolution of the 5 km elevation rasters used in this study. The grounding line layer was downsampled, selecting only 10% of the points using the SQL query `MOD("OID",10)=0`. This effectively selected only points with OID numbers divisible by 10. These points were

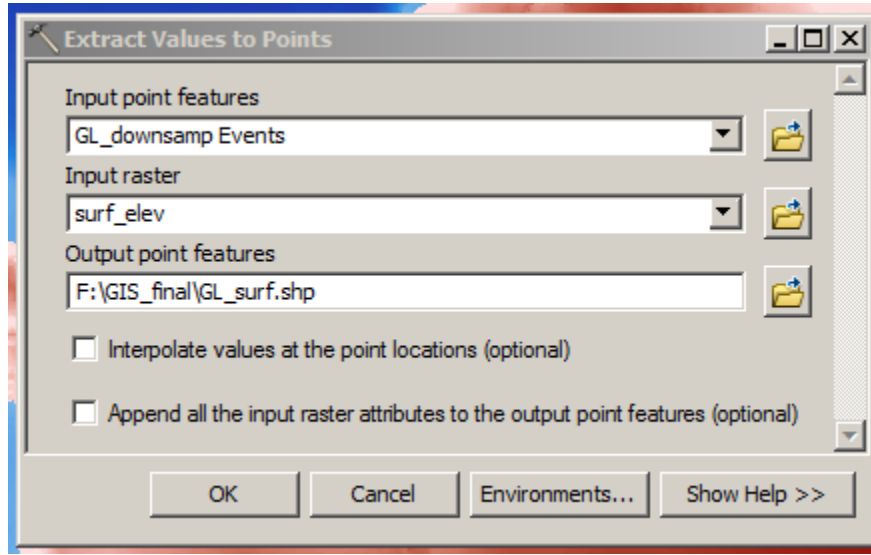


Figure 2: Extraction Tool.

then exported to a database file and added as XY data. By default, the points are symbolized with 4-pt font and an outline, which obscured the structure of the grounding line. Grounding line points were symbolized with 1-pt black points to obtain the working map shown in Fig. 1.

Surface elevations along the grounding line were obtained using the “Extract Values to Points” tool. Inputs were the downsampled grounding line points and the surface raster layer, as shown in Fig. 2. The point extraction process was repeated for bed elevations and ice velocities along the grounding line. The resulting layers, `GL_surf.shp`, `GL_bed.shp`, and `GL_vel.shp` then contained elevations and ice speeds in their respective attribute tables. The simplest method of extracting the data from the attribute tables was to “select all,” right-click on the layer, and choose “Copy Records For Selected Features,” then paste the tables into Microsoft Excel. Unnecessary columns were eliminated.

### 3.5 Import feature names

The `glacier_name.xlsx` file described in Sec. 2.4 was imported into ArcMap with the “Add XY Data” tool and labels were turned on. The resulting map is shown in Fig. 3.

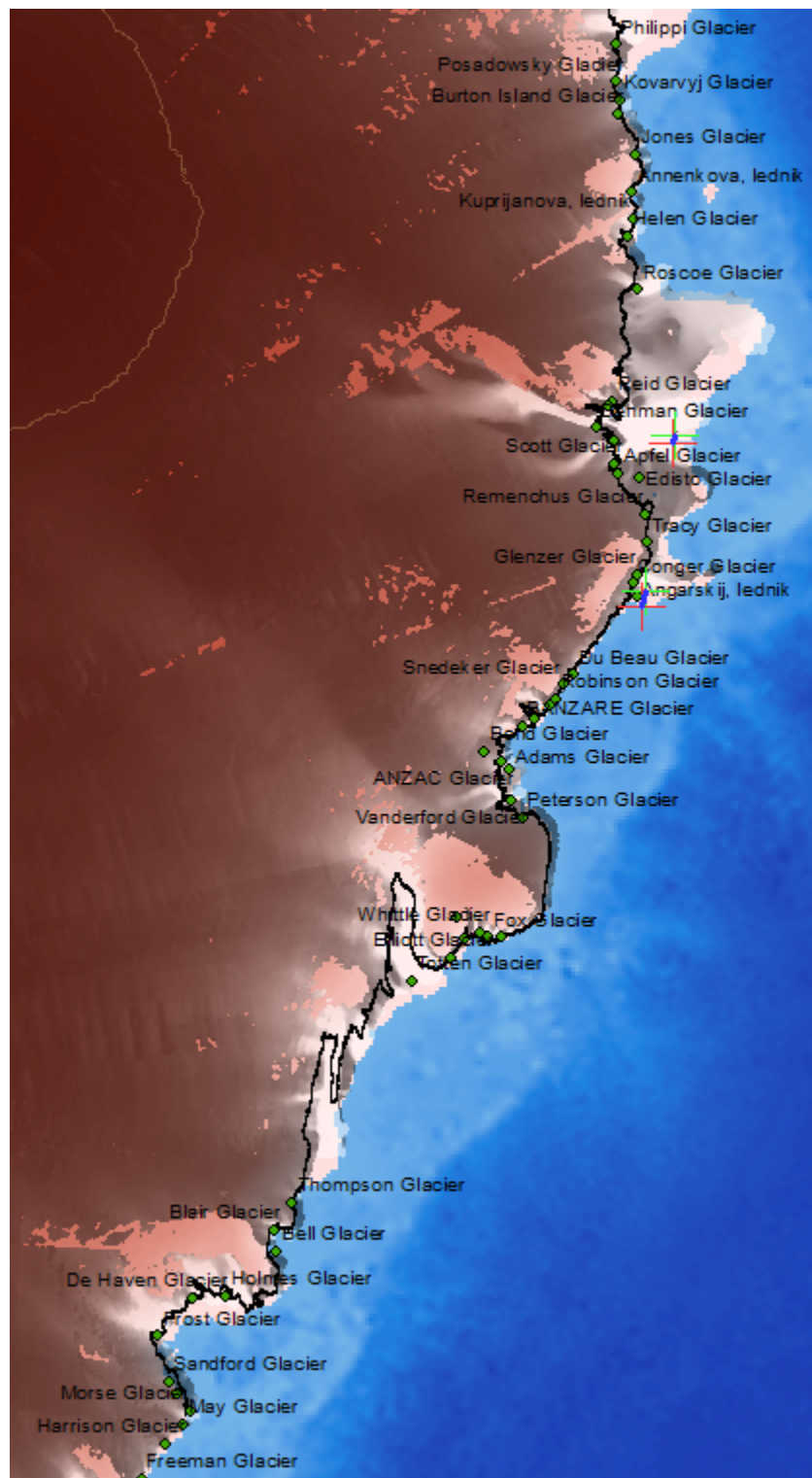


Figure 3: Region of interest.

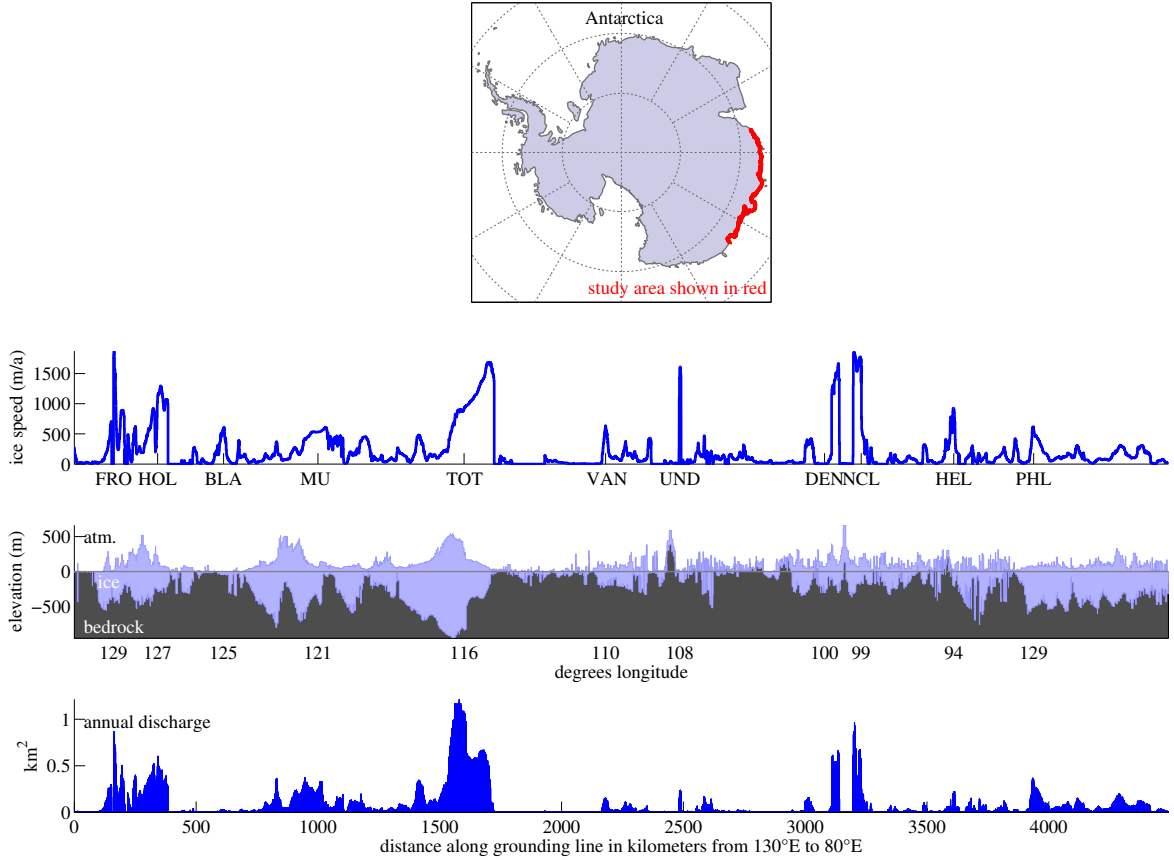


Figure 4: Postprocessing results produced by the MATLAB script provided in the Appendix. Glacier abbreviations correspond to those listed in Table 1.

## 4 Postprocessing

ArcGIS data were postprocessed using the MATLAB script provided in the Appendix. Outlet glacier bed elevations, surface elevations, velocities, and corresponding flow rates are presented in Fig. 4.

## 5 Results

Flow rates and geometries were calculated for the major outlet glaciers in the study area. Ice thickness, speed, and bed elevation were taken as their nominal values along the grounding line. Calculated results are shown in Table 1. Although Totten is not the fastest-moving glacier in the region, it has an annual discharge an order of magnitude



glacier name	lat	lon	width (km)	thickness (m)	bed (m)	speed (m/a)	discharge (km <sup>3</sup> /a)
Frost (FRO)	67.1°S	129°E	4	416	-396	1802	3
Holmes (HOL)	66.8°S	126.9°E	51	367	-255	1005	18
Blair (BLA)	66.8°S	124.5°E	40	40	-39	383	1
Moscow (MU)	67.0°S	121°E	83	533	-416	500	22
Totten (TOT)	66.8°S	116.3°E	188	761	-527	1101	130
Vanderford (VAN)	66.6°S	110.4°E	24	258	-195	440	3
Underwood (UND)	66.7°S	107.9°E	9	138	-133	1295	2
Denman (DEN)	66.8°S	99.4°E	31	391	-205	1411	17
Northcliffe (NCL)	66.7°S	98.7°E	34	347	-215	1698	20
Helen (HEL)	66.65°S	93.8°E	22	162	-104	757	3
Philippi (PHL)	66.8°S	88.3°E	10	583	-512	570	3

Table 1: Names of primary glaciers and related ice shelves under investigation. Glacier thickness, bed elevations, and speeds are presented as their nominal values.

greater than other glaciers in the region, owing primarily to its width.

Pritchard *et al.* found that thinning rates of Totten ice shelf are significantly greater than any other ice shelf in the region, and suggested that this may be related to the thickness of the ice here—that along coastal Antarctica, thick ice is currently experiencing the highest thinning rates. However, Pritchard *et al.* also identified Holmes and Conger as undergoing notable thinning and by the measurements presented here, Holmes and Conger are not considerably thick. Furthermore, Moscow University Ice Shelf is nearly as thick as Totten, but Pritchard *et al.* found no significant thinning here.

A currently unproven theory regarding the sources of glacial earthquakes suggests that the events are more likely to occur on glaciers that are thick relative to their width. Geometries calculated here neither support nor counter this theory, as only eight glacial earthquakes have been centered in the region, and seven of them came from Adams glacier, which has a geometry similar to several other glaciers in the region.

Sources of error may include the inexact georeferencing of the ice velocity layer, the somewhat subjective identification of ice stream margins, and the assumption that ice moves as plug flow, perpendicular across the grounding line, and that any given parcel of ice will only cross the grounding line once.

## References

- [1] L.A. Stearns and G.S. Hamilton. Thinning and acceleration of East Antarctic outlet glaciers. In *AGU Fall Meeting Abstracts*, volume 1, page 08, 2007.
- [2] HD Pritchard, SRM Ligtenberg, HA Fricker, DG Vaughan, MR Van den Broeke, and L. Padman. Antarctic ice-sheet loss driven by basal melting of ice shelves. *Nature*, 484(7395):502–505, 2012.
- [3] M. Nettles and G. Ekström. Glacial earthquakes in Greenland and Antarctica. *Annual Review of Earth and Planetary Sciences*, 38:467–491, 2010.
- [4] J.L. Bamber and R.A. Bindshadler. An improved elevation dataset for climate and ice-sheet modelling: validation with satellite imagery. [http://nsidc.org/data/docs/daac/nsidc0076\\_antarctic\\_5km\\_dem.gd.html](http://nsidc.org/data/docs/daac/nsidc0076_antarctic_5km_dem.gd.html), 1997.
- [5] J. Mouginot Rignot, E. and B. Scheuchl. Ice Flow of the Antarctic Ice Sheet. [http://nsidc.org/data/docs/measures/nsidc0484\\_rignot/index.html](http://nsidc.org/data/docs/measures/nsidc0484_rignot/index.html), 2001.
- [6] H. A. Fricker L. Padman Brunt, K. M. and S. O’Neel. Antarctic grounding line mapping from differential satellite radar interferometry. [http://nsidc.org/data/docs/agdc/nsidc0469\\_brunt/index.html](http://nsidc.org/data/docs/agdc/nsidc0469_brunt/index.html), 2011.
- [7] J. Mouginot Rignot, E. and B. Scheuchl. ICESat-Derived Grounding Zone for Antarctic Ice Shelves. [http://nsidc.org/data/docs/measures/nsidc0498\\_rignot/index.html](http://nsidc.org/data/docs/measures/nsidc0498_rignot/index.html), 2010.
- [8] H. Choi Bindshadler, R. and ASAID Collaborators. High-resolution Image-derived Grounding and Hydrostatic Lines for the Antarctic Ice Sheet. [http://nsidc.org/data/docs/agdc/nsidc0489\\_bindshadler/index.html](http://nsidc.org/data/docs/agdc/nsidc0489_bindshadler/index.html), 2011.
- [9] Scientific Committee on Antarctic Research. Composite Gazetteer of Antarctica. <https://data.aad.gov.au/aadc/gaz/scar/>, 2012.

## Appendix

### 5.1 Georeferencing

Georeferencing steps are depicted in Figures 5 and 6.

### 5.2 Postprocessing script

```
spd = xlsread('gl_speed.xls');  
bed = xlsread('gl_bedelev.xlsx');  
surf = xlsread('gl_surfelev.xlsx');
```

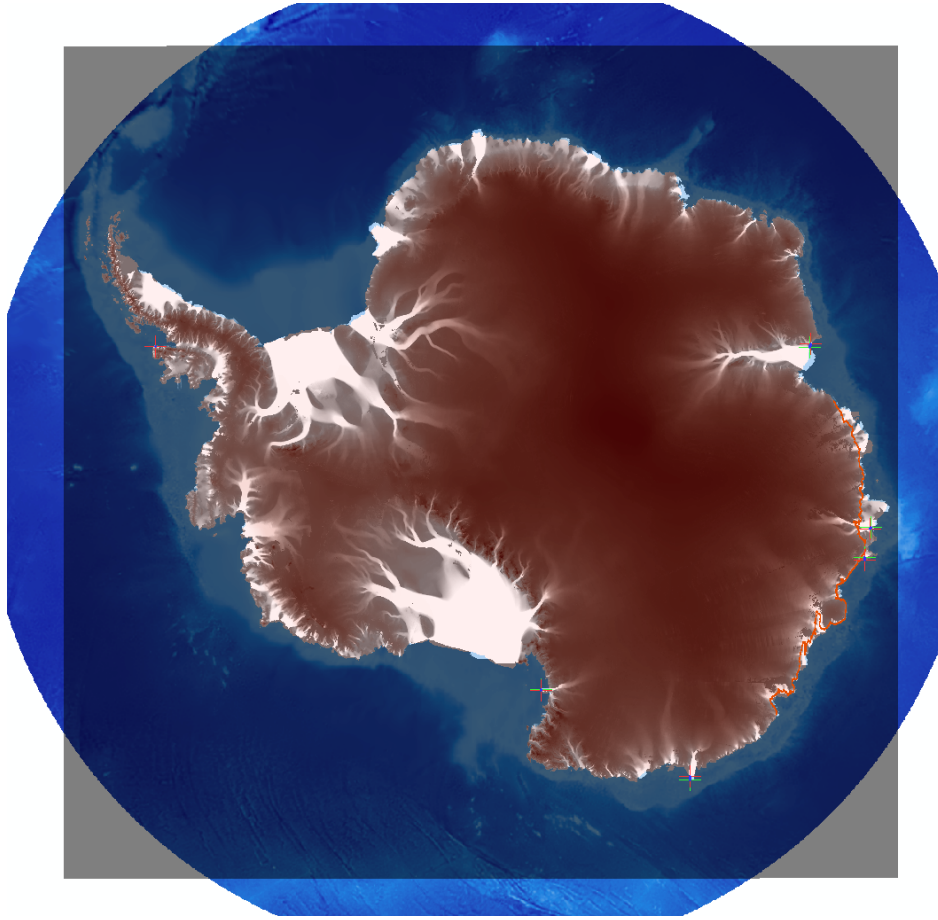


Figure 5: Layers and rectification points shown as + emblems.

```

lat = spd(:,2); % bed and surface files contain redundant lat/lons
lon = spd(:,1);
spd = spd(:,3);
bed = bed(:,3);
surf = surf(:,3);
bed(bed>surf)=0; % eliminates bed-above-surface error

dist = NaN(size(lat)); % preallocate for speed
dist(1)=0;
for n = 1:length(lat)-1
    dist(n+1) = pos2dist(lat(n+1),lon(n+1),lat(n),lon(n),1);
end
dist=cumsum(dist);

% glacier locations:
fro = [-67 129]; % Frost
hol = [-66.77 126.9]; % Holmes

```

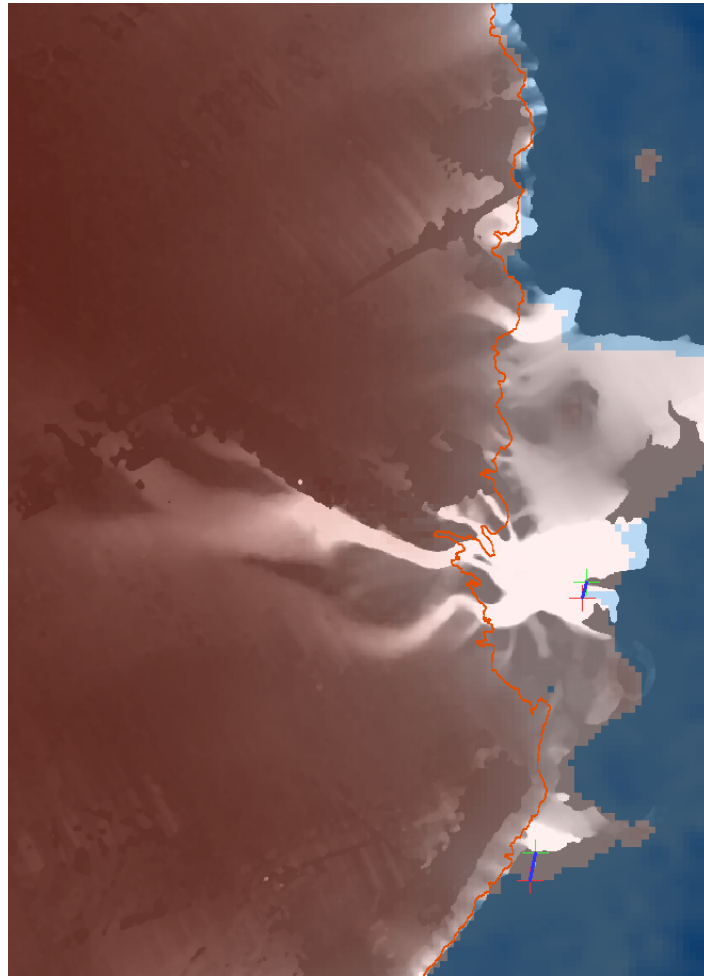


Figure 6: Zoomed-in view of layers after georeferencing the velocity layer. Offset is evident.

```

bla = [-66.75 124.53]; % Blair
mu = [-67 121]; % Moscow University
tot = [-67 116.3]; % Totten
van = [-66.6 110.4]; % Vanderford
und = [-66.66 107.95]; % Underwood
den = [-66.75 99.5]; % Denman
ncl = [-66.7 98.87]; % Northcliffe
hel = [-66.65 93.84]; % Helen
phl = [-66.83 87.92]; % Philippi
featnames = ['FRO'; 'HOL'; 'BLA'; 'MU '; 'TOT'; 'VAN'; ...
             'UND'; 'DEN'; 'NCL'; 'HEL'; 'PHL'];
featlons = [fro(2); hol(2); bla(2); mu(2); tot(2); van(2); ...
            und(2); den(2); ncl(2); hel(2)];
featdists = [161; 342; 613; 1000; 1600; 2181; 2486; 3080; 3230; 3610; 3938];

```

```

figure
set(gcf,'position',[100 100 1400 1000])
subplot(5,1,1:2)
ncpolarm('lat',-65,'grid');
plotm(lat,lon,'r','linewidth',3)
text(0.5,.95,' Antarctica','color','k','units',...
      'normalized','HorizontalAlignment','center')
text(1,.05,'study area shown in red ','color','r',...
      'units','normalized','HorizontalAlignment','right')

subplot(5,1,3)
plot(dist,spd,'b','linewidth',2)
set(gca,'xtick',featdists,'xticklabel',featnames)
axis tight
box off
ylabel('ice speed (m/a)')

subplot(5,1,4)
h1=fill([dist;flipud(dist)],[bed;(min(bed)-10)*ones(size(bed))],...
        [0.3 0.3 .3]); hold on
h2=fill([dist;flipud(dist)],[surf;flipud(bed)],[0.7 0.7 1]);
set(h2,'edgecolor',[0.6 0.6 1]);
plot(dist,zeros(size(dist)),'color',[.5 .5 .5]);
set(gca,'xtick',featdists,'xticklabel',round(featlons))
axis tight
box off
ylabel('elevation (m)')
xlabel('degrees longitude')
text(0,.1,' bedrock','color','w','units','normalized')
text(0,.5,' ice','color','w','units','normalized')
text(0,.9,' atm.','color','k','units','normalized')

subplot(5,1,5)
bar(dist,m22km2((surf-bed).*spd),'b')
axis tight
box off
text(0,.8,' annual discharge','units','normalized')
ylabel('km^2')
xlabel('distance along grounding line in kilometers from...
       130 deg. E to 80 deg E')

```